Die geometry induced heterogeneous morphology of polypropylene inside the die during die-drawing process

Dong Lyu,[1,2] Yingying Sun,[3] Glen Thompson,[4] Ying Lu,[1,*] Philip Caton-Rose,[4] Yuqing Lai,[1] Phil Coates,[4] Yongfeng Men[1,2,*]

[1] State Key Laboratory of Polymer Physics and Chemistry, Changchun Institute of Applied Chemistry, Chinese Academy of Sciences, Renmin Street 5625, Changchun 130022, P. R. China

[2] University of Science and Technology of China, Hefei 230026, P. R. China

[3] ExxonMobil Asia Pacific Research & Development Co., Ltd., 1099 Zixing Road, Minhang District, Shanghai 200241, P. R. China

[4] Polymer Interdisciplinary Research Centre, University of Bradford, Bradford BD7 1DP, UK

Abstract

The morphology distribution of isotactic-polypropylene (iPP) shaped through a die during hot stretching process was investigated via wide-angle X-ray diffraction technique. The evolution of micro-structures in the outer layer (layer closer to the die wall) and the inner layer (layer in the center of die) of die-drawn iPP were both recorded. It turned out that the difference of morphology distribution between outer and inner layers changes with the distance from the die entrance to exit. In general, a larger difference between outer and inner layers could be found at the intermediate deformation region inside the die while such difference disappeared at both of the entrance and exit regions of die. These behaviors could be interpreted as a result of the existence of a heterogeneous distribution of force field inside the die, which was caused by the die geometry and inclination of the drawing force. This work showed that the heterogeneous force field inside the die could be revealed

through analyzing the morphology of a die-drawn sample.

Keywords: die-drawing, isotactic-polypropylene, X-ray, die geometry, orientation.

1. Introduction

Polymer materials as one of the most promising material in the twenty-first century have been widely used in automobile, construction, food package, and lots of other aspects in our daily life [1-3]. However, polymers in isotropic state are normally featured with weak strength limiting their application performance. To reinforce polymeric materials, one can either change the chemical structure by introducing rigid main chains or physically process them into a relatively ideal structure [4-6]. Although the former method could solve this problem fundamentally, it is normally difficult to achieve. Therefore, much attention has been paid on the polymer processing technique. The basic idea of polymer processing is to build a polymer network in which polymer chains are ideally stretched so that each chemical bond could help taking load, yet not too extended to protect the system from peeling apart [4]. There are lots of effective processing methods being well-developed currently, such as die drawing [7-9], extrusion [10-12], spinning [13, 14], rolling [15], etc.

Die drawing defined as a solid-state processing technique, is an approach to draw material billet out of a specially designed die [9, 16-18]. Material is supposed to go through a relative optimal deformation path during this process. The typical processing temperature range chosen for die drawing is 5 ^{o}C~50 ^{o}C below the melting point of the material [16, 19, 20] because the polymer chains are moderately activated under this temperature range. In general, high temperature can help elevate the chain mobility of polymer material and subsequently enhance the processability and lower the cost. Meanwhile, the temperature is not too high, so that the die-drawn polymer sample is able to sustain

its integrity during and after processing. Die-drawing technique is different from solid-state extrusion as well as other drawing techniques [16]. Coates and Ward first systematically illustrated that the schematic extrusion and die drawing paths across the time stress-deformation ratio-strain rate surface, which was further revised by adding the path of free tensile drawing [8].

Since die drawing was invented in 1979 [21], more and more materials, including isotactic polypropylene (iPP) [16, 19, 21-23], polyethylene [20, 24], polyoxymethylene [9, 17], polyether ether ketones [18, 25], and polylactic acid [7, 26], have been confirmed to be suitable for this technique. It was also proven to be applicable for various material geometry, including but not limited to tubular products [20] and multi filaments [20]. Similar to extrusion and wire drawing in which a die was also employed [10, 27-31], a heterogeneous strain-stress distribution was found inside the die area for die-drawing process [32, 33]. Ward *et al.* [32] first analyzed the axial stress distribution as a function of the distance to the die entrance for die-drawing process by using a force-equilibrium approach as well as the von-Mises criterion. They achieved a well-general agreement between the experimental observation and theoretical prediction. A coupled thermomechanical finite element model was also once used to study the detailed temperature, strain, and strain rate distributions during the die-drawing process [33]. However, all these previous results were obtained by theoretically simulation or mathematically calculation which was not intuitive, and lack of the discussion of the influence on the samples.

In current work, the distribution of polymer morphology in a modified mini-die during die-drawing process was analyzed using wide angle X-ray diffraction (WAXD) technique. It turns out that there is an obvious rotation of the favorable orientation direction at the intermediate and die exit region when the scanning direction is perpendicular to the deformation direction. On the contrary, this rotation

could not be found at the die entrance. Besides, similar but different orientation evolution paths were found for inner and outer layers of die-drawn iPP cut along die width. The origin of these morphology variations in the die could be ascribed to the die geometry and the drawing force. During the die-drawing process, the width direction of the sample billets was compressed by the die wall, while along the thickness direction the sample billets were not in contact with the die wall. The force field in the die area along the width direction is therefore mainly induced by two components. One is the drawing force, and the other is the die wall which contributed the compressional force and friction. As a consequence, the heterogeneous distribution of force in the die leads to the different morphology distributions in the different regions of die.

2. Experimental section

2.1 Material information and sample preparation

A commercial iPP with a molecular weight of M_w= 158 900 g mol^{-1} and a polydispersity (M_w/ M_n) of 3.8 provided by ExxonMobil was used for investigation. The melting point of this iPP is about 168 ^oC as measured by using differential scanning calorimeter (DSC) (DSC1 Star^e System (Mettler Toledo Swiss)) technique. For preparing tensile bars, the iPP pellets were first made into standard injection molding bars with a length of 170 mm, a width of 10 mm, and a thickness of 4 mm. In order to fit the width of mini die, the width of injection molded bars were further reduced to 6 mm by using a circular saw suitable for cutting plastics.

2.2 Die-drawing tests

The mini die-drawing setup used in the present work is provided by Professor Coates' laboratory at

the University of Bradford (UK). This setup is characterized with a mini die in which the die exit dimension is 5 mm in thickness and 2 mm in width, respectively. As shown in Fig. 1, this die-drawing setup basically contains three parts, including the drawing system, the temperature system, and the controlling system. The drawing system consists of a sample clamp which is driven by a motor with a drawing speed ranging from 5 to 300 mm min^{-1}. A force sensor is attached on the clamp to monitor the instant load on the sample during drawing. A specially designed mini die, the essence of the die-drawing technique, is the core of the drawing system. This part could induce neck profile at early deformation stage and let the sample bar go through a relative optimal deformation path. A delicate design was employed in the temperature system, which enables independent temperature control of the mini die and the sample oven. A couple of electrical heating bars are embedded in the base of the mini die, while heated air are pumped through the sample oven during the experiment. Thermocouples which are also machined into the mini die and the sample oven, together with Eurotherm temperature controller, realize precise monitoring and controlling on the temperature of each part, respectively. The controlling system enables us to alter the temperature settings and drawing speed both locally and remotely. It could also reflect and record the instant load applied on the sample billets and other related experimental parameters through a self-developed program.

A detailed photo of the die with a die-drawn sample in it can also be seen in the top right of Fig. 1. This rectangular die compressed the sample only on its width direction and the thickness direction of the sample could be considered not effected by the shape of the die during drawing.

In the case of die drawing, tensile bar was first warmed up inside the sample oven for 20 minutes at the preset temperature. Then, the sharpened head of tensile bar out of die was tightened by the clamp and followed by stretching under a certain drawing speed. Two stretching temperatures of 130 ^{o}C and

150 °C were chosen according to the appropriate temperature used in die-drawing process and two drawing speeds of 93 and 300 mm min^{-1} were applied to the tensile tests, respectively. The average sample length inside the die was around 7.5 mm, resulting an average strain rates of 0.2 and 0.7 s^{-1}. After stretching to a certain length, the drawn samples were fixed at their two ends for 20 minutes before taking them out of the die and the clamp.

As depicted in Fig. 2 (a), die-drawn samples were further cut into inner and outer layers along width direction of die. Fig. 2 (b) shows an as cut outer layer on which each deformation area is marked out on the sample layer. X_v represents the vertical distance to the die entrance line, X_h represents the relative position corresponding to the center point of the sample thickness horizontally, and the red point was set as (X_v, X_h) = (0, 0). Sample layers were analyzed horizontally along the thickness direction at the intermediate deformation area (②) and the die exit area (③) as well as vertically along the drawing direction in the middle of each layer starting from the die entrance area.

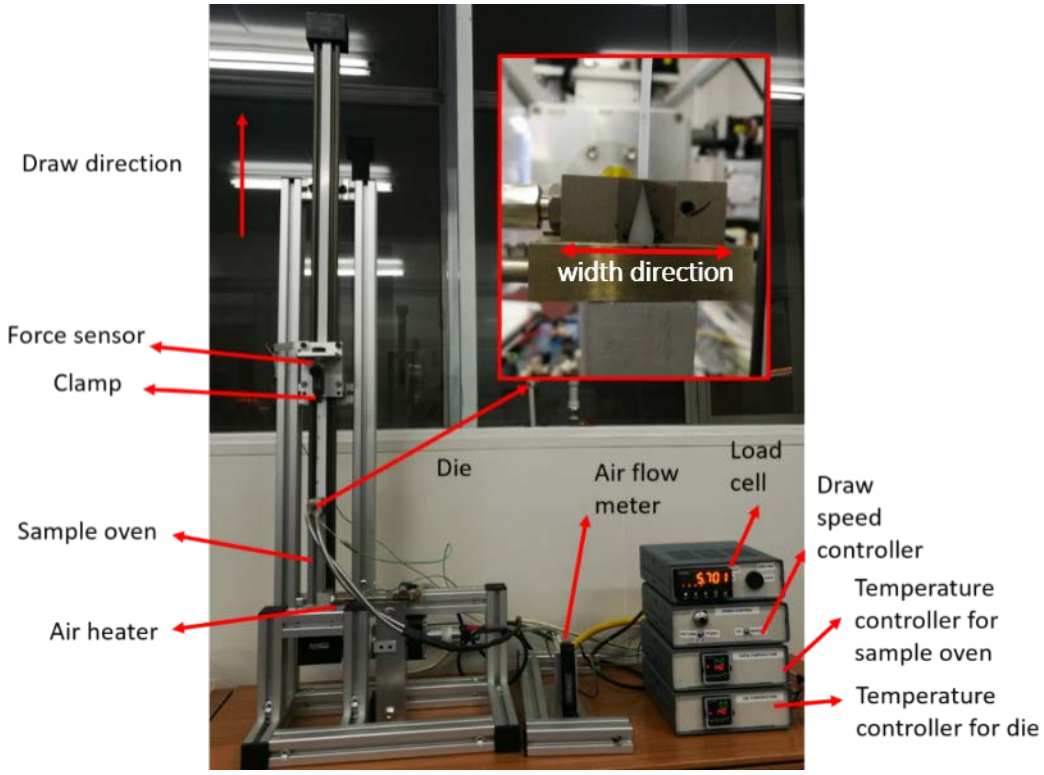

Fig.1. Photograph of mini die-drawing setup. A detailed picture of the die is in the inset.

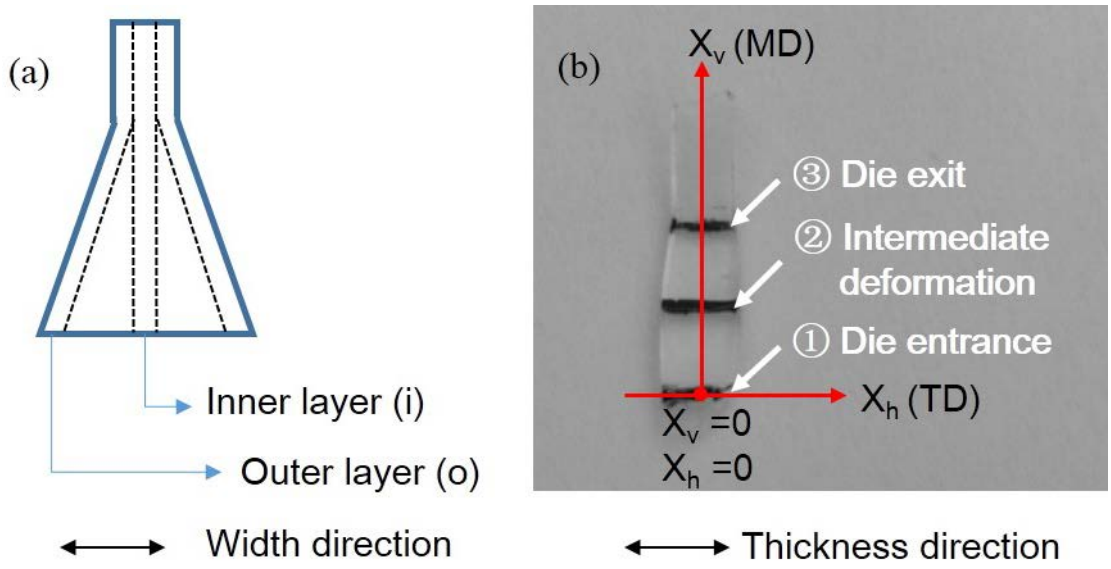

Fig. 2. (a) A front view of a die-drawn sample is given to depict the layers of samples for further X-ray experiments. (b) A photo of the outer layer in which X-ray mapping directions were marked out.

2.3 WAXD experiments

WAXD experiments were performed by using a customized micro-focus WAXD system. A focused Cu Kα X-ray source (GeniX^{3D}, Xenocs SA, France), generated at 50 kV and 0.6 mA, was employed in this setup. The two-dimensional (2D) WAXD patterns were collected by a semiconductor detector with a resolution of 487 pixels × 195 pixels (pixel size =172 μm) (Pilatus100 K, DECTRIS, Swiss) at a sample-to-detector distance of 20.8 mm. The X-ray beam with a spot size of 40 × 60 μm^2 was first positioned at the red point ((X_v, X_h) = (0, 0)) of each as cut layer, and the samples were then moved along the direction of X_v at a step length of 0.5 mm. Then the samples were also moved along the direction of X_h from left to right with a step length of 0.4 mm at the position shown as the upper two black lines in Fig. 2(b). Due to the thickness change during drawing, which makes the measurement range not always an exact multiple of 0.4, a smaller step was applied at the edge of each sample layer and the position of each point was recalculated accordingly. The acquisition time for each pattern was

60 s.

Moreover, the Hermanns formula [34] was applied to evaluate the orientation degree of polymer chains within crystalline phase, which is expressed as

$$S_{hkl} = \frac{3<cos^2\phi_{hkl}>-1}{2} \quad (1)$$

where ϕ_{hkl} denotes the angle between the flow direction and the normal vector of the lattice plane (*hkl*). Additionally, orientation parameter $\cos^2\phi_{hkl}$ can be achieved from azimuthal scattering intensity distribution by the following equation

$$cos^2\phi_{hkl} = \frac{\int_0^{\pi/2} I_{hkl}(\phi)cos^2\phi sin\phi d\phi}{\int_0^{\pi/2} I_{hkl} sin\phi d\phi} \quad (2)$$

where $I_{hkl}(\phi)$ describes the scattering intensity along the angle ϕ. And ϕ can be obtained by using Polanyi equation [35]

$$cos\phi_{hkl} = cos\theta_{hkl} cos\psi \quad (3)$$

where θ_{hkl} denotes the Bragg scattering angle, ψ is the azimuthal angle along the Debye circle. In the case of a perfect orientation of the lattice plane with its normal in the plane of equator, the order parameter *S* is equal to -0.5. For an isotropic sample, the order parameter *S* is usually presented as 0. Therefore, the orientation parameter of (hk0) planes can vary in the range from 0 to -0.5 when the alignment of molecular chains from its isotropic state to perfectly oriented one along the polar direction, as the normal of such planes are normally perpendicular to chain direction.

3. Results and Discussion

3.1 WAXD mapping results along the thickness direction

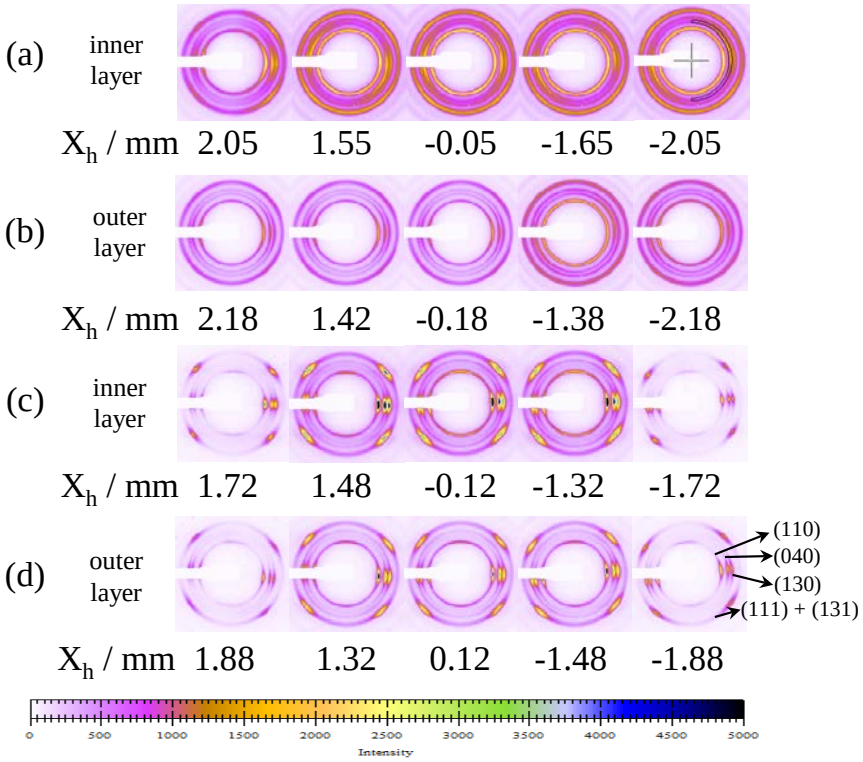

Fig. 3. Selected 2D WAXD patterns along thickness direction for inner layers and outer layers of samples drawn with a speed of 300 mm min^{-1} at 130 ºC. (a) and (b) present the mapping results along the thickness direction at the intermediate deformation zone, while (c) and (d) show the results at the die exit area, corresponding to ② and ③ in Fig. 2 (b), respectively. (Drawing direction: vertical.)

Fig. 3 presented the selected two-dimensional WAXD patterns along thickness direction (TD) for the inner layer and the outer layer of iPP sample after drawn at 130 ºC with a speed of 300 mm min^{-1}. In general, only the characteristic diffraction peaks of α form appeared during the whole drawing process, and the corresponding lattice planes were marked out in Fig. 3. Focusing on the evolution of WAXD patterns in Fig. 3 (a), one could notice that the orientation direction of molecular chains in die-drawn iPP changed with X_h. It indicated that the distribution of distinct microstructures existed along the thickness direction in the inner layer at the intermediate region of die drawn iPP. Meanwhile, the similar tendency was also observed in the outer layer at the same region of drawn iPP sample (Fig. 3 (b)). In the case of the inner and outer layers of drawn iPP in the region of die exit (Fig. 3(c) and (d)),

both layers followed the same trend as found in the intermediate region that the different orientation directions of molecular chains occurred as varying X_h. However, much stronger orientation of molecular chains can be distinguished in the latter case as evidenced by the highly concentrated arcs along the horizontal direction. In a word, a slight but obvious rotation of the maximum scattering position could be found in these WAXD patterns for a certain layer as altering the X_h. Such a change was independent of layers.

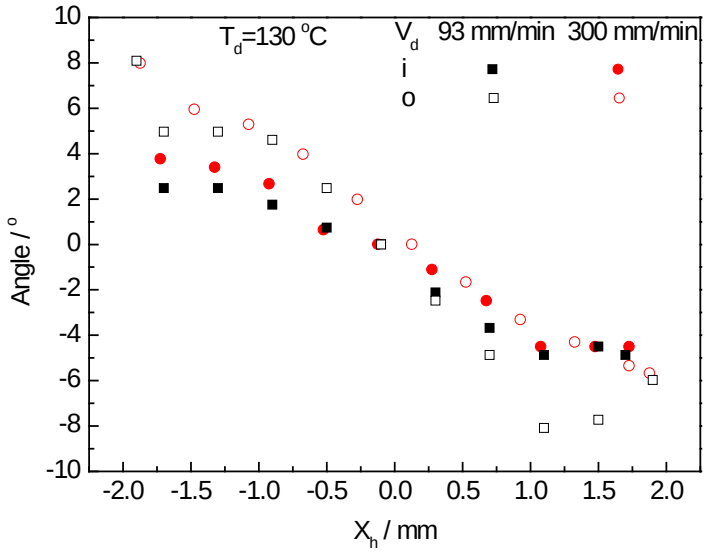

Fig. 4. Rotation angle along thickness direction for inner layers (i) and outer layers (o) at the die exit region of die drawn samples after being stretched at 130 °C with different speeds.

In order to give a more detailed illustration of this rotation, ring integrals were employed. As presented in Fig. 3, the integral area covered the principal part of the diffraction ring of the crystallographic plane of $(040)_\alpha$ starting from -90 ° to 90 ° in a counterclockwise direction. An integral angle of 360 ° is unnecessary, since the diffraction pattern is symmetrical. The most intensive point of each integrated curve represented the most favorable orientation direction. Fig. 4 depicts the relative location of maximum scattering intensity of the crystallographic plane of $(040)_\alpha$ with respect to the perpendicular direction to the drawing direction using the die-exit region WAXD patterns of die drawn

iPP after being stretched under different speeds. In Fig. 4, the rotation angle is quite obvious for all layers even under different drawing speeds, indicating that a rotated force was applied to the sample and this force was not strongly affected by drawing speed. Furthermore, the rotation angle changed gradually rather than abruptly when the value of X_h increased. It manifests that this deviation from the direction which is perpendicular to the drawing direction (the angle of 0 ^{o}) is not simply induced by the necking profile of the samples. To alter the preferential orientation direction in this case, a force in the sample layer plane is required. As mentioned above, the width of sample is compressed by the die wall while the thickness is not. In other words, the rotation of molecular chains along thickness direction seemed not to be caused by the shape of the die. Besides, the width of sample also suffered from friction which is induced by the compression of the die wall. And these two forces should have different influence on the outer layers and the inner layers, because of the different distance to the die wall. The consistent behavior of these two layers again indicated that the rotation was unlikely to be caused by the die wall. Therefore, the possible reason for this phenomenon is the tilted drawing force.

To figure out whether this force could influence the orientation degree of molecular chains of iPP along thickness direction during die drawing, the order parameter $S_{(040)\alpha}$ at different regions of drawn iPP was calculated through equations of (1), (2), and (3). The azimuthal integration area along the crystallographic plane of $(040)_\alpha$ was still set as -90^o to 90^o, and then, the azimuthal angle was corrected by setting the azimuth of the most intensive diffraction point as 90^o before calculation. Because the reference direction should be set as stretching direction which is normally 90^o with respect to the most intensive diffraction point of crystallographic (hk0) planes. The corresponding results were depicted in Fig. 5. For the intermediate deformation zone, one can find a large fluctuation of $S_{(040)\alpha}$ in both of inner and outer layers as changing the X_h. This behavior could be regarded as a result of the skin-core

structure induced by injection molding process [36]. At this deformation stage, the initial microstructure was partially preserved and hence detected by the X-ray techniques. In the case of the die exit area, the molecular chains clearly showed a much better orientation degree as evidenced by lower values of $S_{(040)\alpha}$ compared to ones in the intermediate deformation region. Simultaneously, the skin-core structure in this region was nearly eliminated with respect to the near constant $S_{(040)\alpha}$ values at different X_h. The variation tendency of $S_{(110)\alpha}$ is similar to the one of $S_{(040)\alpha}$. Here, we could recognize that the orientation degree of molecular chains along thickness direction at a certain deformation region was hardly affected by the tilted drawing force in the die.

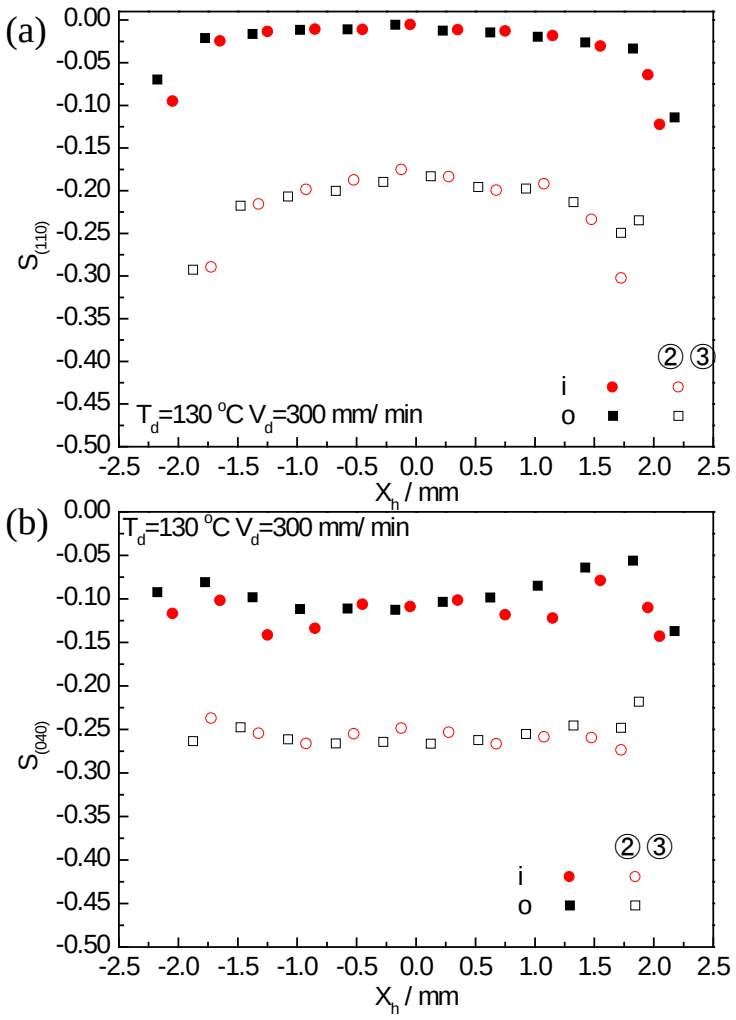

Fig. 5. (a) orientational order parameter of $(110)_\alpha$ planes comparison along thickness direction for

inner layer(i) and outer layer(o) of drawn iPP at different deformation zones in the die after stretched with a speed of 300 mm min^{-1} at 130 ^{o}C. (b) orientational order parameter of $(040)_{\alpha}$ planes comparison along thickness direction. (② and ③ represent the intermediate deformation zone and the area at the die exit, corresponding to Fig. 2.)

Based on all these results above, it could be easily deduced that even though the samples were not compressed along the thickness direction, the deformation behavior of samples along this direction was still not homogeneous. The influence of the skin-core structures of iPP induced by injection molding process had been excluded for resulting in the rotation angle of molecular chains along the thickness direction at different regions of die drawn samples. Therefore, the potential reason for causing such uneven evolution of microstructures in the die drawn iPP was proposed to be the tilted drawing force. Although the essence of this mini die-drawing setup was to try to merely alter one dimension of the sample (the width of sample in this case), it was inevitable that both of the width and thickness would change in practical operation. The thickness of the sample outside the die was slightly smaller than its original thickness, inducing a smaller effective grip range, especially when the sample head for gripping was made by die-drawing process. Fig. 6 depicted a half part of the inner structure of the die and in the middle of which was the compressional die wall. The distribution of the drawing force along the thickness direction in the die is marked out by red arrows. Apparently, the force direction tilts from the two open sides to the middle part due to the difference in the thicknesses of different part of the sample (undeformed vs deformed). The thickness direction of iPP sample was not in contact with the die wall but suffered from the tilted drawing force, and consequently the molecular chains oriented along different directions at different positions along the thickness direction.

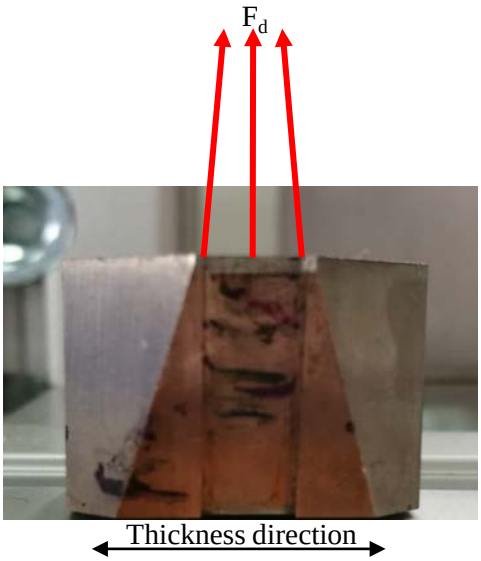

Fig. 6. A schematic of the drawing force distribution inside the die along the thickness direction. F_d represents the drawing force.

3.2 WAXD mapping results along drawing direction

For the purpose of detecting the development of microstructures of drawn iPP samples along the stretching direction, the as cut samples were also mapped along this direction. To eliminate the influence of the drawing force inclination as much as possible, we chose only to measure vertically along the center of each layer (as schematized in Fig. 2 (b) along X_v). Selected 2D WAXD patterns of these mapping processes are shown in Fig. 7. WAXD patterns obtained at the inner layer of iPP drawn at 130 ^oC are chosen as examples. As can be seen, the patterns at X_v of 0 started from nearly isotropic ones, which was caused by injection-molding process [36], and the diffraction rings gradually turned into arcs with increasing X_v. It reveals that well-oriented structures along the drawing direction had been introduced after the iPP sample has been processed through the die.

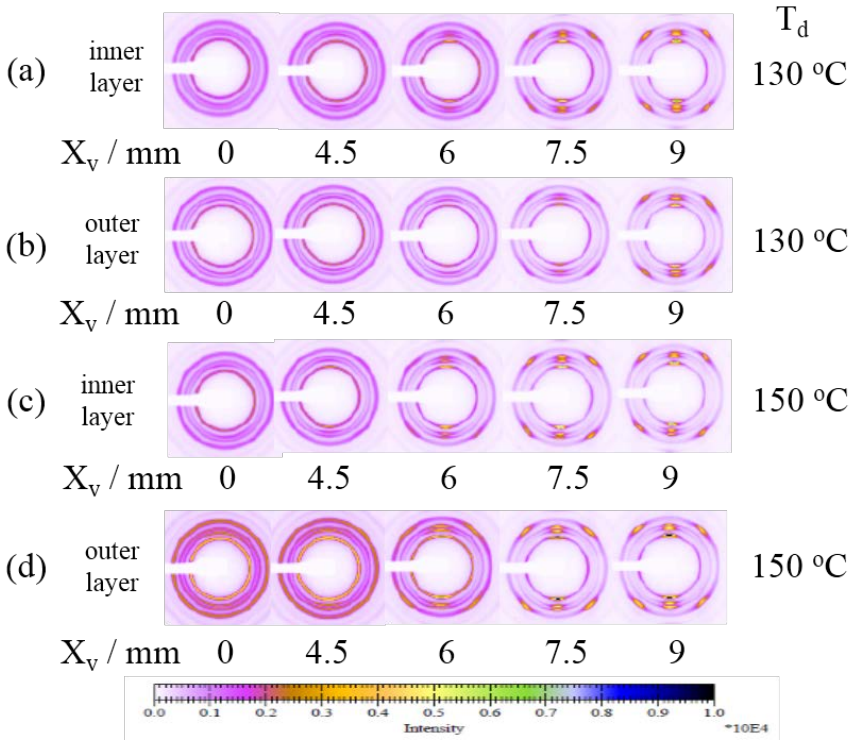

Fig. 7. Selected 2D WAXD patterns along drawing direction for inner layers and outer layers of samples drawn with a speed of 93 mm min^{-1} at different temperatures. (drawing direction: horizontal.)

In order to understand the orientation degree of molecular chains along the deformation direction, Fig. 8 gives the results of $S_{(040)\alpha}$ for both inner and outer layers of die drawn iPP after stretched at different conditions. The azimuthal integration area along the crystallographic plane of $(040)_\alpha$ in this case was set as 0^o to 180^o since the stretching direction was horizontal. Firstly, it was easy to find out that the $S_{(040)\alpha}$ was reduced with increasing X_v in all cases matching the results displayed in Fig. 7. The orientation evolution could be divided into three regions according to the slope of the curves, namely the orientation efficiency. The boundaries between adjacent stages were marked out in Fig. 2 (b). These three regions were defined as the early deformation stage region in which the sample had not necked down and was still tightly in contact with the die wall, the intermediate deformation region in which the sample had already necked down yet not left the die wall, and the final deformation stage in which the sample left the die wall near the die exit.

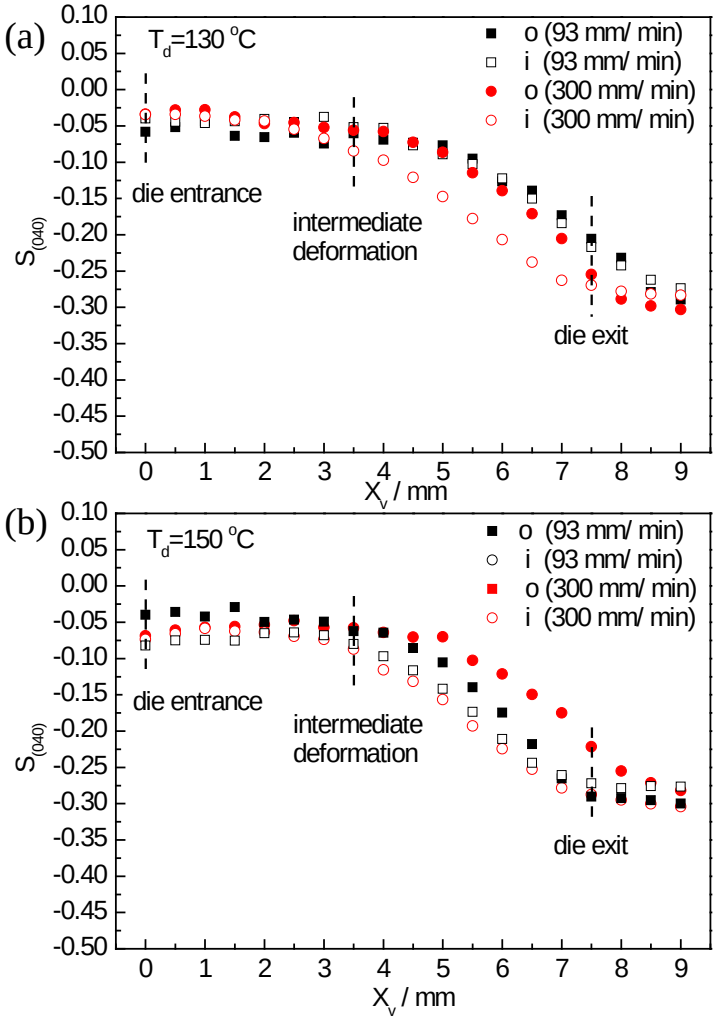

Fig. 8. orientational order parameter of $(040)_\alpha$ planes versus X_v in outer (o) and inner layers (i) of iPP drawn at different conditions.

Focusing on these three regions, it was quite obvious that the slope in both of the early and the final deformation stages is small, indicating that the change of the orientation degree is sluggish. On the contrary, at the intermediate deformation stage a steeper slope was found which was an evidence of a quick adjustment of molecular chains along the drawing direction. Secondly, different evolution paths occurred for the inner and outer layers of drawn iPP at different conditions. In the case of iPP deformed at 130 °C under the speed of 93 mm min^{-1}, the orientation degree of molecular chains in the inner and

outer layer were almost the same at a certain X_v. Nevertheless, this phenomenon disappeared in the rest of the deformation cases. For example, the situations in the inner and outer layers in iPP deformed at 130 ºC under the speed of 300 mm min^{-1} were almost the same at the early deformation stage while the inner layer exhibited a better orientation degree comparing to the outer layer when X_v extended beyond the intermediate deformation stage. The difference between layers continued to increase until the sample reached the final deformation stage, and then the inner layer and the outer layer tended to share the similar orientation parameter in the end. Moreover, this difference could be enlarged when increasing the drawing speed or elevating the deformation temperature.

Fig. 9 presented the evolution of the orientational order parameter of $(110)_\alpha$ planes as a function of X_v. The basic evolution tendency was almost the same as the one of the $(040)_\alpha$ planes and could be divided into three deformation regions by the orientation efficiency as well. But the difference between different layers did not exhibit apparent temperature dependency. This could be a result of different parent-daughter structure evolution at different temperatures [37]. Unlike the $(040)_\alpha$-lattice plane, the parent lamellae and daughter lamellae would take different positions on the diffraction ring of $(110)_\alpha$-lattice plane which would be an obstruction on calculating the orientation degree by the Hermanns method. In other words, the calculated results of $(110)_\alpha$-lattice plane could not depict the chain orientation along the force direction as accurate as the ones of $(040)_\alpha$-lattice plane. Thus, only the orientational order parameter of $(040)_\alpha$ planes was focused in the later discussion.

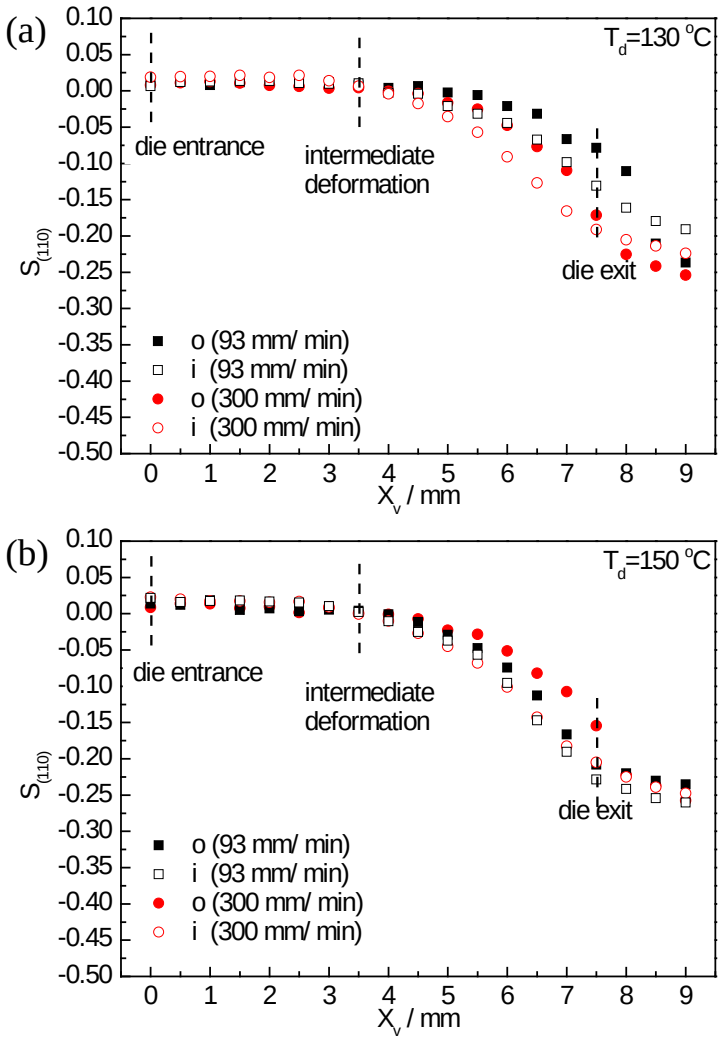

Fig. 9. The orientational order parameter of $(110)_\alpha$ planes versus X_v in outer (o) and inner layers (i) of iPP drawn at different conditions.

Here, the mechanism behind these behaviors discussed above could be interpreted by stress-induced melting and recrystallization process inside the die during die drawing process. As being well-established in recent years, block slippage within the crystalline lamellae takes place first, followed by the stress-induced fragmentation and recrystallization starting at certain strain determined by the stability of crystalline blocks and the state of entangled amorphous network for semi-crystalline polymer upon stretching [38-40]. Under a sufficient stress, the original crystallites can be mechanically

molten to form new crystallites which are composed with molecular chains oriented along the deformation direction. Thus, such melting and recrystallization process of polymers during stretching is essentially determined by the stress endured by each crystallites [41]. It can be envisioned that it is a gradual process rather than a uniform change for all crystallites being melted and recrystallized. Only those crystallites suffered sufficient high stress can be first melted and then recrystallized [41].

For die drawing process, the different orientation degrees of molecular chains in iPP occurred in the inner and outer layers in the intermediate deformation stage of die means that the original crystallites in these two layers were borne with different stress. It indicates that an uneven force distribution existed inside the die during die drawing process. Indeed, such hypothesis had also been proposed by Ward *et al.* by using a force equilibrium approach [32] and finite element simulation [33], respectively. The former work mainly concentrated on the axial stress and die wall pressure evolution from the die entrance to the die exit [32]. An increase in the axial stress was found as the material proceeded inside the die and this increase became greater with increasing billet speed. If the material was in contact with the die wall during the whole die-drawing process, the die wall pressure would generally decrease to a minimum value before increasing towards the die exit. But for the case similar to the present work in which the material left the die wall somewhere before the die exit, the pressure would keep decreasing until zero. These results were also well agreed by experimental results. Maps of strain rate distribution inside profiled dies was depicted based on the finite element simulation method [33], which indicated that the strain, strain rate and consequently the stress was uneven distributed not only along the drawing direction but also across the tangent direction inside the die.

Based on our experimental results and results suggested by Ward *et al.* [32, 33], the force distribution inside the die is depicted in Fig. 10. The compression force (N) perpendicular to the die

wall could be orthogonally decomposed into two independent components N_h and N_v. The friction (f) which was along the die wall and partially determined by N could also be orthogonally resolved into f_h and f_v. N_h could help the orientation of the polymer chains while f_h could impede this effect. Since the value of f_h is smaller than the one of N_h, the overall effect of these two forces was in favor of the orientation. On the contrary, N_v and f_v both had an opposite direction comparing to the drawing force, thus they could become an obstruction. In summary, the compression force and friction could be transformed into F_h along the width direction which was in favor of the orientation along the machine direction and F_v which could hinder the orientation.

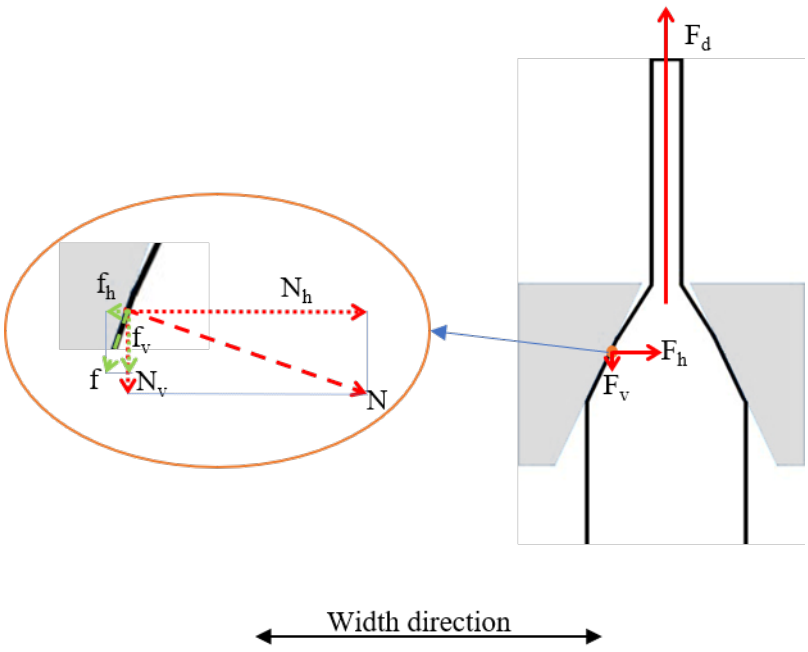

Fig. 10. A schematic graph of the force distribution along the width direction, including the drawing force (F_d), the compression force (N), the friction (f), as well as the overall effect of the latter two along horizontal direction F_h and along drawing direction F_v.

Similar to the die wall pressure evolution proposed by Ward *et al.* [32] , F_h and F_v was supposed to decrease from the die entrance to the die exit. Besides, it is obvious that, for a given X_v position, F_h was the same for outer and inner layers, while F_v became weaker as it went through the outer layers

to inner layers. A weaker orientation was thus always achieved in the outer layers than the inner layers inside of the die at the same X_v. Moreover, better chain mobility at higher temperature made molecular chains more sensitive to the force difference between the outer and inner layers, while elevating drawing speed could effectively enlarge the force difference between different layers. Therefore, the difference between outer and inner layers in the intermediate region of die occurred more visible when the drawing temperature or speed increased. One thing should be noticed that similar as along the thickness direction, the inclination of the drawing force was also expected along the width direction. In other words, the drawing force F_d was different for each layer. But the influence of it on the orientation degree variation could be neglected, since it was proved not to affect the orientation efficiency in the previous discussion.

In a whole view of the different behavior occurred in die-drawn iPP along X_v, the features of these variations could be highlighted as follows. At the early deformation stage, the sample had not necked down and was still in its elastic deformation zone, in which the polymer chains could easily recover to its original state once the drawing force was removed. This recovery behavior was considered to be responsible for the starting plateau of the orientation degree evolution in different layers of iPP samples. With increasing X_v, the samples started to experience the permanent deformation process attributing to the plastic flow. In this deformation zone, the molecular chains adjusted themselves quickly and led to an evident improvement of the orientation degree under the effect of the drawing force and the compressional die wall. Once the sample left the die wall near the die exit, contribution of the compression force was no longer expected, and the drawing force solely oriented the molecular chains resulting a relative low speed of orientation.

As for the asynchronous evolution behavior between outer and inner layers, it could be a result of

the competition between F_d, F_v and F_h. Since F_v was smaller at the inner layers than the outer layers, it was reasonable that an inferior orientation degree could be found in the latter. F_v was the largest at the die entrance but the difference between the outer and inner layers could not be observed until the sample necked down. As samples necking down, the effect of F_v would gradually wear off and eventually disappeared after sample left the die wall. Thus, we could observe the difference of the orientation degree between inner and outer layers first became larger and then slowly decreased. Finally, at some point out of the die, the orientation degree of outer and inner layers would be the same again.

Combining all the results, the molecular chain segments within crystallites were effectively oriented during the die drawing process. A rotated orientation preference could be found along the thickness direction inside the die. Since the sample was not compressed along this direction, the only possible reason was the inclined drawing force. In the case of orientation degree along the deformation direction, it could be divided into three regimes by the different slopes at each deformation stage. The difference of orientation degree between inner and outer layers first increased and then decreased, and finally was eliminated. Such different variation could be understood as a consequence of the change of F_v which represented the effective vertical force induced by the die geometry.

4. Conclusion

To conclude the current work, wide-angle X-ray diffraction technique was employed to investigate the microstructure evolution in samples die-drawn at different conditions. The various morphologies found in the die-drawn samples could be interpreted as a result of different levels of stress-induced melting and recrystallization under different sufficient stress, which is caused by the drawing force

inclination and the die geometry induced heterogeneous force field inside the die. The die-drawing process could effectively elevate the orientation degree of the molecular chains. A slight different orientation direction was found along the thickness direction which was not compressed by the die wall but was originated from the inclination of the drawing force. Furthermore, the die-drawing process could be divided into three deformation zones corresponding to different variation tendency of orientation along the deformation direction. At the early deformation stage, the sample was still at elastic region, thus the orientation degree almost stayed the same. As necking down, molecular chains oriented quickly with the help of drawing force and the die wall. It was also the beginning that the difference between inner and outer layers appeared. After the sample left the die wall, the orientation evolved by drawing force alone and the uneven force field distribution induced by the shape of the die disappeared, resulting in a slow orientation development and a reduction of the difference. Clearly, the morphology evolution of iPP samples was clarified and interpreted during the die-drawing process in this work.

Acknowledgements

This work is supported by the National Natural Science Foundation of China (21704102 and 51525305), Newton Advanced Fellowship of the Royal Society, United Kingdom (NA 150222) and ExxonMobil. We thank Dr. Ran Chen at CIAC who developed the MATLAB codes for data processing.

References

[1] Y. Lu, Y. Y. Sun, L. Li, Y. F. Men, Influence of propylene-based elastomer on stress-whitening for impact copolymer, J. Appl. Polym. Sci. 134 (2017) 44747.

[2] J. Li, Y. X. Ji, J. R. Chang, N. Tian, L. X. Song, L. Chen, L. B. Li, Structural origin of fast yielding-

strain hardening transition in fluoroelastomer f2314, Polymer 119 (2017) 107-111.

[3] R. A. C. Deblieck, D. J. M. van Beek, K. Remerie, I. M. Ward, Failure mechanisms in polyolefines: The role of crazing, shear yielding and the entanglement network, Polymer 52 (2011) 2979-2990.

[4] A. E. Zachariades, W. T. Mead, R. S. Porter, Recent developments in ultra-orientation of polyethylene by solid-state extrusion, Chem. Rev. 80 (1980) 351-364.

[5] K. L. Jin, E. K. Leitsch, X. Chen, W. H. Heath, J. M. Torkelson, Segmented thermoplastic polymers synthesized by thiol-ene click chemistry: Examples of thiol-norbornene and thiol-maleimide click reactions, Macromolecules 51 (2018) 3620-3631.

[6] D. P. Jones, D. C. Leach, D. R. Moore, Mechanical properties of poly(ether-ether-ketone) for engineering applications, Polymer 26 (1985) 1385-1393.

[7] J. F. Li, Z. Q. Li, L. Ye, X. W. Zhao, P. Coates, F. Caton-Rose, M. Martyn, Structure evolution and orientation mechanism of long-chain-branched poly (lactic acid) in the process of solid die drawing, Eur. Polym. J. 90 (2017) 54-65.

[8] P. D. Coates, P. Caton-Rose, I. M. Ward, G. Thompson, Process structuring of polymers by solid phase orientation processing, Sci. China Chem. 56 (2013) 1017-1028.

[9] A. K. Taraiya, M. S. Mirza, J. Mohanraj, D. C. Barton, I. M. Ward, Production and properties of highly oriented polyoxymethylene by die-drawing, J. Appl. Polym. Sci. 88 (2003) 1268-1278.

[10] S. Rungruangsuparat, S. Patcharaphun, N. Sombatsompop, Materials modification and die design for minimizing internal melt distortions of glass fiber/pp co-extrudates, Polym. Test. 57 (2017) 184-191.

[11] T. Shimada, A. E. Zachariades, M. P. C. Watts, R. S. Porter, Push-pull extrusion: A new approach to solid-state deformation illustrated with high density polyethylene, J. Appl. Polym. Sci. 26 (1979)

1309-1326.

[12] K. Shigematsu, K. Imada, M. Takayanagi, Formation of kink bands by compression of extrudate of solid linear polyethylene, J. Polym. Sci., Part B: Polym. Phys. 13 (1975) 73-86.

[13] A. Rizvi, Z. K. M. Andalib, C. B. Park, Fiber-spun polypropylene/polyethylene terephthalate microfibrillar composites with enhanced tensile and rheological properties and foaming ability, Polymer 110 (2017) 139-148.

[14] D. Gregor-Svetec, F. Sluga, High modulus polypropylene fibers. I. Mechanical properties, J. Appl. Polym. Sci. 98 (2005) 1-8.

[15] J. Jia, D. Raabe, Evolution of crystallinity and of crystallographic orientation in isotactic polypropylene during rolling and heat treatment, Eur. Polym. J. 42 (2006) 1755-1766.

[16] P. D. Coates, I. M. Ward, Die drawing - solid-phase drawing of polymers through a converging die, Polym. Eng. Sci. 21 (1981) 612-618.

[17] P. S. Hope, A. Richardson, I. M. Ward, Manufacture of ultrahigh-modulus poly(oxymethylenes) by die drawing, J. Appl. Polym. Sci. 26 (1981) 2879-2896.

[18] A. Richardson, F. Ania, D. R. Rueda, I. M. Ward, F. J. Baltá Calleja, The production and properties of poly(aryletherketone) (peek) rods oriented by drawing through a conical die, Polym. Eng. Sci. 25 (1985) 355-361.

[19] A. K. Taraiya, A. Richardson, I. M. Ward, Production and properties of highly oriented polypropylene by die drawing, J. Appl. Polym. Sci. 33 (1987) 2559-2579.

[20] A. G. Gibson, I. M. Ward, High stiffness polymers by die-drawing, Polym. Eng. Sci. 20 (1980) 1229-1235.

[21] P. D. Coates, I. M. Ward, Drawing of polymers through a conical die, Polymer 20 (1979) 1553-

1560.

[22] C. E. Chaffey, A. K. Taraiya, I. M. Ward, Orientation in polypropylene sheets produced by die-drawing and rolling, Polym. Eng. Sci. 37 (1997) 1774-1784.

[23] I. A. Polec, P. J. Hine, M. J. Bonner, I. M. Ward, D. C. Barton, Hydro and thermal stability of die drawn wood polymer composites in comparison to solid wood, Compos. Sci. Technol. 72 (2012) 1436-1442.

[24] A. G. Gibson, I. M. Ward, The manufacture of ultrahigh modulus polyethylenes by drawing through a conical die, J. Mater. Sci. 15 (1980) 979-986.

[25] D. R. Rueda, F. Ania, A. Richardson, I. M. Ward, F. J. B. Calleja, X-ray-diffraction study of die drawn poly(aryletherketone) (peek), Polym. Commun. 24 (1983) 258-260.

[26] A. T. Morita, M. S. Toma, M. A. De Paoli, Low cost capillary rheometer, transfer molding and die-drawing module, Polym. Test. 25 (2006) 197-202.

[27] S. H. Wen, T. J. Liu, J. D. Tsou, 3-dimensional finite-element analysis of polymeric fluid-flow in an extrusion die .1. Entrance effect, Polym. Eng. Sci. 34 (1994) 827-834.

[28] R. Ahmed, R. F. Liang, M. R. Mackley, The experimental-observation and numerical prediction of planar entry flow and die swell for molten polyethylenes, J. Non-Newton. Fluid 59 (1995) 129-153.

[29] T. R. Salamon, D. E. Bornside, R. C. Armstrong, R. A. Brown, The role of surface-tension in the dominant balance in the die swell singularity, Phys. Fluids 7 (1995) 2328-2344.

[30] P. Y. Wu, L. M. Huang, T. J. Liu, A simple-model for heat-transfer inside an extrusion die, Polym. Eng. Sci. 35 (1995) 1713-1724.

[31] S. H. Zhang, X. D. Chen, J. Zhou, D. W. Zhao, Upper bound analysis of wire drawing through a twin parabolic die, Meccanica 51 (2016) 2099-2110.

[32] F. A. Motashar, A. P. Unwin, G. Craggs, I. M. Ward, Analytical and experimental-study of the die drawing of circular rods through conical dies, Polym. Eng. Sci. 33 (1993) 1288-1298.

[33] I. M. Ward, J. Mohanraj, D. C. Barton, Analysis and design of profiled dies for polymer wire die drawing process, Plast. Rubber Compos. 37 (2008) 301-304.

[34] P. Hermanns, P. Platzek, Beiträge zur kenntnis des deformationsmechanismus und der feinstruktur der hydratzellulose, Kolloid Z. 88 (1939) 68-72.

[35] M. Polanyi, The X-ray fiber diagram, Z. Phys. 7 (1921) 149-180.

[36] M. R. Kantz, H. D. Newman, F. H. Stigale, The skin-core morphology and structure-property relationships in injection-molded polypropylene, J. Appl. Polym. Sci. 16 (1972) 1249-1260.

[37] R. G. Alamo, G. M. Brown, L. Mandelkern, A. Lehtinen, R. Paukkeri, A morphological study of a highly structurally regular isotactic poly(propylene) fraction, Polymer 40 (1999) 3933-3944.

[38] Y. F. Men, J. Rieger, G. Strobl, Role of the entangled amorphous network in tensile deformation of semicrystalline polymers, Phys. Rev. Lett. 91 (2003) 095502.

[39] Z. Y. Jiang, Y. T. Wang, L. L. Fu, B. Whiteside, J. Wyborn, K. Norris, Z. Wu, P. D. Coates, Y. F. Men, Tensile deformation of oriented poly(epsilon-caprolactone) and its miscible blends with poly(vinyl methyl ether), Macromolecules 46 (2013) 6981-6990.

[40] Y. T. Wang, Z. Y. Jiang, L. L. Fu, Y. Lu, Y. F. Men, Stretching temperature dependency of lamellar thickness in stress-induced localized melting and recrystallized polybutene-1, Macromolecules 46 (2013) 7874-7879.

[41] Y. Lu, R. Chen, J. Y. Zhao, Z. Y. Jiang, Y. F. Men, Stretching temperature dependency of fibrillation process in isotactic polypropylene, J. Phys. Chem. B 121 (2017) 6969-6978.